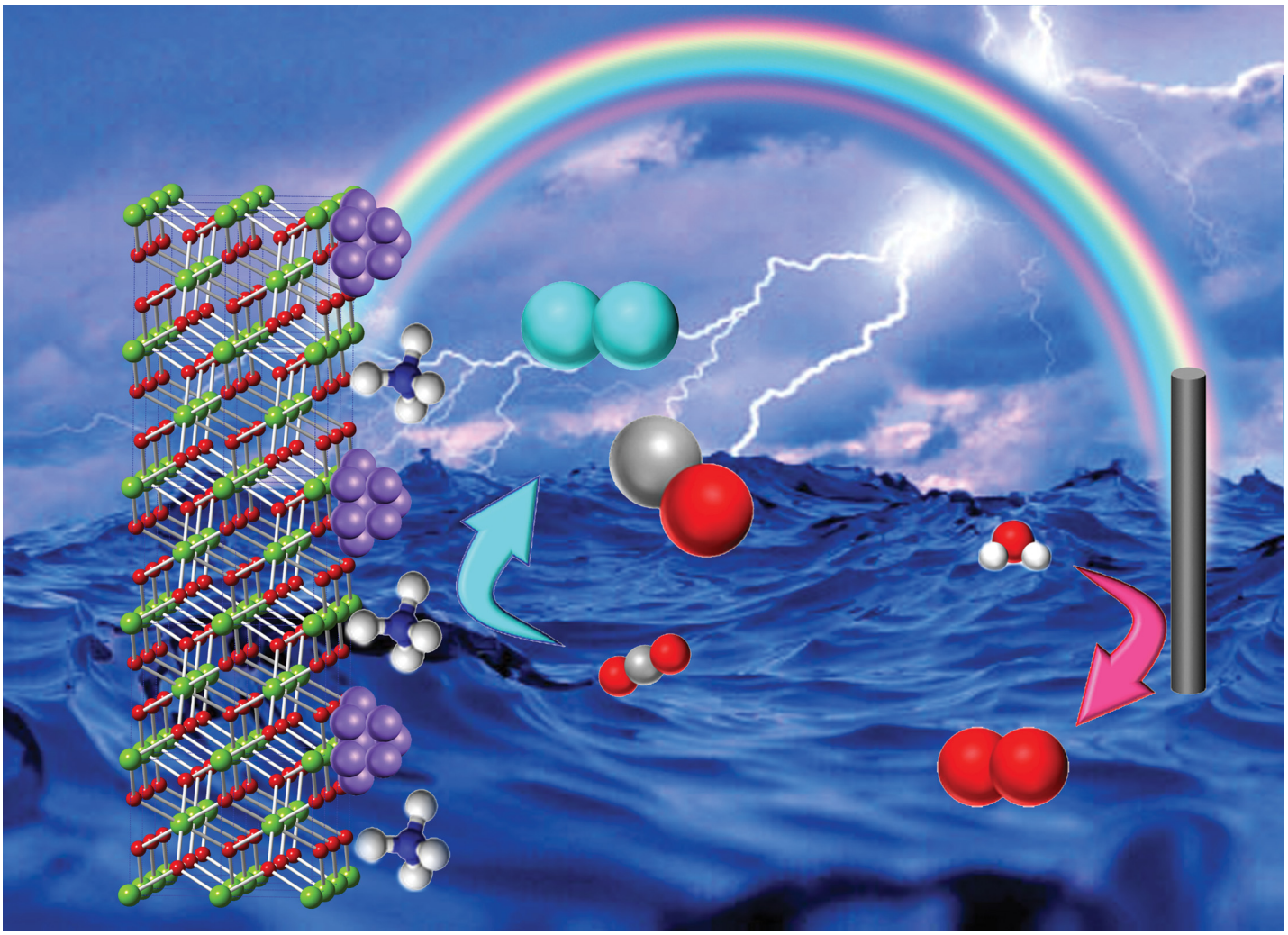

Showcasing research from Professor Hiroaki Tada's laboratory, Department of Applied Chemistry, Faculty of Science and Engineering, Kindai University, Osaka, Japan

Ammonium ion-promoted electrochemical production of synthetic gas from water and carbon dioxide on a fluorine-doped tin oxide electrode

Sn nanoparticles on fluorine-doped tin oxide act as an electrocatalyst for CO_2 reduction to efficiently and stably produce synthetic gas from water and carbon dioxide with the reaction rate drastically enhanced by the addition of ammonium ions.

As featured in:

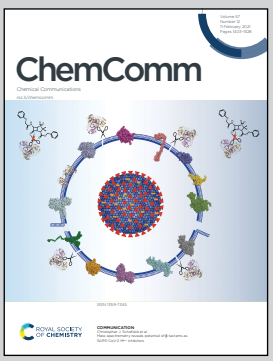

See Hiroaki Tada *et al.*, *Chem. Commun.*, 2021, **57**, 1438.

ROYAL SOCIETY OF CHEMISTRY

rsc.li/chemcomm

Registered charity number: 207890

ChemComm

COMMUNICATION

View Article Online
View Journal | View Issue

Cite this: *Chem. Commun.*, 2021, **57**, 1438

Received 11th December 2020,
Accepted 11th January 2021

DOI: 10.1039/d0cc08040c

rsc.li/chemcomm

Ammonium ion-promoted electrochemical production of synthetic gas from water and carbon dioxide on a fluorine-doped tin oxide electrode†

Shin-ichi Naya,[a] Hisayoshi Yoshioka[b] and Hiroaki Tada *[b]

In situ **generated Sn nanoparticles on fluorine-doped tin oxide act as an electrocatalyst for the CO_2 reduction reaction to efficiently and stably produce synthetic gas from water and carbon dioxide with the reaction rate drastically enhanced by the addition of ammonium ions.**

The CO_2 reduction reaction (CO_2-RR) to hydrocarbons and oxygenated compounds is the key technology to solving the issues of climate change and energy deficiency through carbon recycling.[1] However, these multi-electron reduction processes are usually accompanied by high overpotential with low selectivity.[2] On the other hand, synthetic gas consisting of H_2 and CO is a basic feedstock for various important chemical processes including C1 chemistry and the Fischer–Tropsch process. At present, synthetic gas is mainly produced by gasification of fossil fules at a high temperature with a large quantity of energy consumed. The electrochemical production of synthetic gas from water and CO_2 by utilizing renewable electricity can be a fascinating green process,[3] while surplus electricity can also be effectively used as the energy source. Since the pioneering work by Fujishima and co-workers,[4] the research on the electrochemical production of synthetic gas is currently in rapid progress.[5–7] Fortunately for this purpose, the standard electrode potential of CO_2 reduction to CO (standard reduction potential $E^0 = -0.104$ V, eqn (1)) is close to that of water reduction ($E^0 = 0$ V, eqn (2)), where the potential is shown with respect to the standard hydrogen electrode potential (SHE). CO_2 dissolved in water is partly hydrated to generate H_2CO_3 ($K = 1.7 \times 10^{-3}$ at 25 °C, eqn (1)).

$$CO_2(aq.) + H_2O(l) \leftrightarrow H_2CO_3(aq.) \quad (1)$$

Further, H_2CO_3 can be ionized in two steps (eqn (2) and (3)).

$$H_2CO_3(aq.) + H_2O(l) \leftrightarrow HCO_3^-(aq.) + H_3O^+(aq.),\ pK_{a1} = 6.37 \quad (2)$$

$$HCO_3^-(aq.) + H_2O(l) \leftrightarrow CO_3^{2-}(aq.) + H_3O^+(aq.),\ pK_{a2} = 10.32 \quad (3)$$

Since only molecular CO_2 undergoes reduction,[8] the electrochemical CO_2-RR should be carried out in a near-neutral electrolyte. On the other hand, the electrochemical CO_2-RR needs protons and electrons, and is usually carried out under acidic conditions, where the solubility of CO_2 in water decreases. In this study, to solve this trade-off, the electrochemical CO_2-RR was performed on a fluorine-doped tin oxide (FTO) electrode using NH_4^+ ions with a great affinity for FTO as a proton donor under near-neutral conditions, while highly active bulk-metal electrodes including mainly Ag and Cu besides Au, Ni, Sn, Zn have been developed so far (Table S1, ESI†). Recent theoretical work has shown that the optimal bulk pH of the electrolyte solution for CO_2-RR should be close to 7.[9] A CO_2-RR on a metal oxide electrode was performed for the first time using an FTO electrode in acidic electrolyte solution, and the transient generation of CO and steady generation of H_2 were confirmed.[10] Also, an Sn–SnO_x-coelectrodeposited titanium electrode was reported to show much higher faradaic efficiency for CO_2 reduction to CO and HCOOH than an SnO_2 electrode with a native oxide layer.[11] On the contrary, the electrochemical CO_2-RR at the metal Sn electrode[12–15] and the Sn–Cu bimetallic electrode[16] yields HCOOH as a major product. Although Li, Sun and co-workers have reported that the electrochemical CO_2-RR using a carbon supported Cu(core)–SnO_2(shell) nanocatalyst yields H_2 and HCOOH at the SnO_2 thickness = 1.8 nm and CO and H_2 at SnO_2 thickness = 0.8 nm,[17] the selective synthetic gas production has not been achieved.

Here, we report the stable and efficient electrochemical production of synthetic gas from water and CO_2 on an FTO electrode in a near-neutral electrolyte solution containing NH_4^+ ions by using a three-electrode two-compartment cell with the

[a] *Environmental Research Laboratory, Kindai University, 3-4-1, Kowakae, Higashi-Osaka, Osaka 577-8502, Japan*

[b] *Graduate School of Science and Engineering, Kindai University, 3-4-1, Kowakae, Higashi-Osaka, Osaka 577-8502, Japan. E-mail: h-tada@apch.kindai.ac.jp; Fax: +81-6-6727-4301; Tel: +81-6-6721-2332*

† Electronic supplementary information (ESI) available. See DOI: 10.1039/d0cc08040c

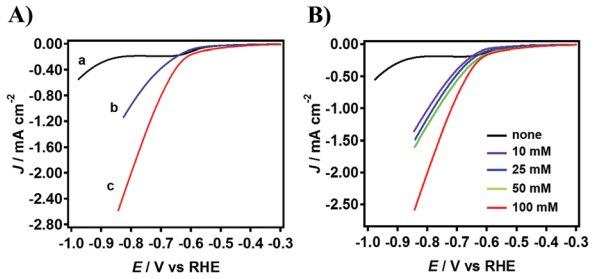

Fig. 1 (A) LSVs for FTO electrode: (a) in 0.1 M Na_2SO_4 aq. after 30 min CO_2 bubbling (pH 5.5), (b) in 0.1 M Na_2SO_4–0.1 M $NaHCO_3$ aq. (pH 8.0), (c) in 0.1 M Na_2SO_4–0.1 M $NaHCO_3$ aq. containing 0.1 M $(NH_4)_2SO_4$ after 30 min CO_2 bubbling (pH 7.7). (B) LSVs for FTO electrode in 0.1 M Na_2SO_4–0.1 M $NaHCO_3$ aq. containing various concentrations of $(NH_4)_2SO_4$ after 30 min CO_2 bubbling.

structure of glassy carbon (GC, anode) | 0.1 M $(NH_4)HCO_3$ aq. (pH 6.7) | Nafion | 0.1 M $(NH_4)HCO_3$ aq. (pH 6.7) | FTO (cathode), Ag/AgCl (reference).

Liner sweep voltammograms (LSVs) were measured for the FTO electrode in the range of electrode potential (E) from 0 to −0.9 V *vs.* reference hydrogen electrode (RHE) (Fig. 1A). In the 0.1 M Na_2SO_4 aq. with CO_2 bubbling, only a small current flows in the potential range. In 0.1 M Na_2SO_4–0.1 M $NaHCO_3$ aq. after 30 min of CO_2 gas bubbling, the cathodic current due to reduction(s) involving the CO_2-RR flows at E < *ca.* −0.7 V. Strikingly, the addition of $(NH_4)_2SO_4$ to the electrolyte solution causes a drastic increase in the current.

Further, LSVs were recorded for the FTO electrode in 0.1 M Na_2SO_4–0.1 M $NaHCO_3$ aq. containing various concentrations of $(NH_4)_2SO_4$ ($[(NH_4)_2SO_4]$) after 30 min of CO_2 bubbling (Fig. 1B and Fig. S1, ESI†). The cathodic current increases with increasing $[(NH_4)_2SO_4]$ in the range below 100 mM. Evidently, the NH_4^+ ion acts as a promoter to remarkably enhance the electrochemical reduction reaction(s).

X-ray diffraction measurements were carried out for the FTO electrode before and after electrolysis in 0.1 M Na_2SO_4–0.1 M $NaHCO_3$ aq. after 30 min of CO_2 bubbling (Fig. 2A). FTO possesses diffraction peaks at 2θ = 33.89°, 38.97°, and 51.78° indexed as the diffraction from the crystal planes of SnO_2(101), (111), and (211), respectively (ICDD 01-075-2893). After the

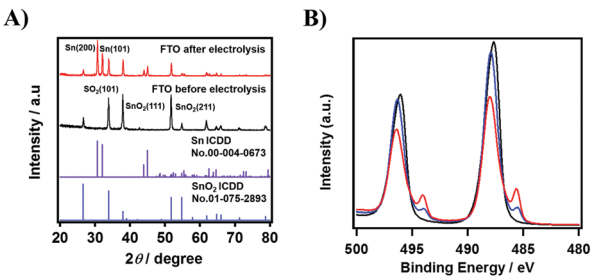

Fig. 2 (A) XRD patterns of FTO electrode before and after 30 min electrolysis at E = −0.9 V *vs.* RHE in 0.1 M Na_2SO_4–0.1 M $NaHCO_3$ aq. (B) XP spectra of FTO electrodes before (black), after 30 min electrolysis in 0.1 M Na_2SO_4–0.1 M $NaHCO_3$ aq. (blue), and after 30 min electrolysis in 0.1 M Na_2SO_4–0.1 M $NaHCO_3$–0.1 M $(NH_4)_2SO_4$ aq. (red).

electrolysis, new peaks appear at 2θ = 30.65° and 32.02° assignable to the diffraction from the (200) and (101) planes of the metallic Sn crystal (ICDD 00-004-0673).

As shown in the Sn3d-X-ray photoelectron (XP) spectra (Fig. 2B), FTO possesses two signals observed at binding energies (E_B) at 487.6 eV and 496.1 eV due to the emissions from the $3d_{5/2}$ and $3d_{3/2}$ orbitals of SnO_2. The electrolysis in 0.1 M Na_2SO_4–0.1 M $NaHCO_3$ without $(NH_4)_2SO_4$ at E = −0.9 V *vs.* RHE for 30 min induces new signals at $E_{B,3d_{5/2}}$ = 485.5 eV and $E_{B,3d_{3/2}}$ = 493.9 eV assignable to the corresponding emissions from metallic Sn,[18] which are intensified by the electrolysis with 0.1 M $(NH_4)_2SO_4$ aq. After the CO_2-RR, the O1s-XP signal at 527.7 eV significantly weakens, while the F1s-XP signal around 685 eV disappears (Fig. S2, ESI†). These results are also consistent with the partial reduction of the FTO surface to form metallic Sn NPs on the surface. As a result, the FTO electrode changed from colourless to brown (Fig. S3, ESI†). Scanning electron microscopy (SEM) images show that particles with a size of ∼200 nm are observed on the surface of FTO after electrolysis at E = −0.9 V *vs.* RHE for 30 min (Fig. S4, ESI†).

A two-compartment three-electrode cell having the structure of GC | 0.1 M $(NH_4)HCO_3$ aq. (pH 6.7) | Nafion | 0.1 M $(NH_4)HCO_3$ aq. (pH 6.7) | FTO, Ag/AgCl was constructed, and for comparison, the electrolyte solution was replaced by 0.1 M $NaHCO_3$ aq. The flow cell was driven at a CO_2 flowing rate of 100 mL min^{-1}. Only H_2 and CO (or synthetic gas) were detected as the gaseous products by gas chromatography, and quantified under a CO_2 flow with a constant rate of 100 mL min^{-1} with the current traced simultaneously. In the 0.1 M $NaHCO_3$ electrolyte cell, the current density (J) gradually increases from 0.7 mA cm^{-2} at the electrolysis time (t_{el}) = 0 to 1.3 mA cm^{-2} at t_{el} = 1 h (Fig. 3A). Also, CO and H_2 are produced with constant rates of 28 μmol h^{-1} and 45 μmol h^{-1}, respectively. The faradaic efficiency (η) was calculated by eqn (4) as a function of t_{el}.

$$\eta = 2N(t)/(\int I(t)\mathrm{d}t/F) \quad (4)$$

where $N(t)$ is the mole number of CO or H_2 produced at $t_{el} = t$, and F is the Faraday constant.

Thus, the metallic Sn NPs formed on FTO (Sn/FTO) at the initial stage of electrolysis catalyze the electrochemical reduction reactions. The η value of CO is almost constant ∼30%, while the value of H_2 decreases from 58% at t_{el} = 0 to 44% at t_{el} = 1 h (Fig. 3B). Interestingly, the replacement of the electrolyte with 0.1 M $(NH_4)HCO_3$ aq. gives rise to a drastic increase in the current. The J slowly increases from 1.7 mA cm^{-2} to reach a constant of 2.4 mA cm^{-2} at t_{el} >30 min (Fig. 3C). Also, CO and H_2 are produced with constant rates of 51 μmol h^{-1} and 95 μmol h^{-1}, respectively. The η values of CO and H_2 generation are almost constant with ∼30% and 55%, respectively (Fig. 3D). In each electrolyte cell, the total Faradaic efficiency remains in the range of 80–90% probably because of the existence of liquid-phase product(s) such as formic acid.[15] However, ^{1}H-NMR measurements failed to detect no product of which the concentration may be too low. In this manner, a drastic enhancement of synthetic gas from water and CO_2 can be induced by the addition of NH_4^+ ions to the electrolyte

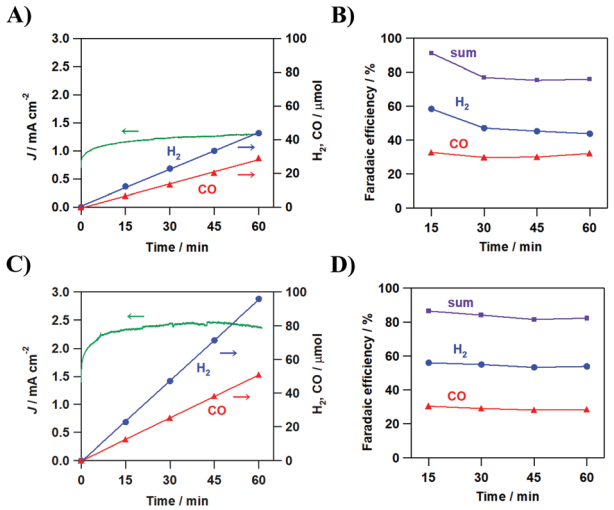

Fig. 3 (A) Chronoamperometry curves and time evolution of gaseous products in a three-electrode cell with the structure of GC | 0.1 M $NaHCO_3$ aq. (pH 6.8) | Nafion | 0.1 M $NaHCO_3$ aq. (pH 6.8) | FTO, Ag/AgCl under CO_2 flow with a constant rate of 100 mL min^{-1}. The potential of FTO electrode was maintained at −0.9 V *vs.* RHE. Each pH is the value at the initial state. (B) Faradaic efficiency of CO and H_2 generation under the same conditions. (C) Chronoamperometry curves and time evolution of gaseous products in a three-electrode cell with the structure of GC | 0.1 M $(NH_4)HCO_3$ aq. (pH 6.7) | Nafion | 0.1 M $(NH_4)HCO_3$ aq. (pH 6.7) | FTO, Ag/AgCl under CO_2 flow with a constant rate of 100 mL min^{-1}. The potential of FTO electrode was maintained at −0.9 V *vs.* RHE. (D) Faradaic efficiency of CO and H_2 generation under the same conditions.

solution, while steady generation of O_2 at the GC anode is also confirmed. The pHs of the anolyte and the catholyte after t_{el} = 4 h were 6.9 and 6.8, respectively. This is ascribable to the buffering action of HCO_3^- ions since the pHs of the anolyte and the catholyte lowered to 2.7 and 5.4, respectively, after t_{el} = 4 h without HCO_3^- ions. Further to check whether SO_4^{2-} ions affect the CO_2-RR properties or not, $(NH_4)_2SO_4$ was used instead of $(NH_4)HCO_3$ as the supporting electrolyte (Fig. S6, ESI†). Remarkable effects by the NH_4^+ ion addition similar to those shown in Fig. 3 with $(NH_4)HCO_3$ are observed, indicating that the influence of SO_4^{2-} ions on the cell performances is small. Recently, the electrochemical production of synthetic gas on a boron-doped diamond electrode has been reported with the faradaic efficiencies of CO ~28% and H_2 ~42% in $KClO_4$ aq.[19]

To gain insight into the action of NH_4^+ ions on the electrochemical CO_2-RR on FTO, FTO particles were synthesized (see the ESI,† for details), and the adsorption properties for NH_4^+ ions were studied. The adsorption behaviour apparently follows the Langmuir model (Fig. 4A). From the Langmuir plot, the saturated adsorption amount (Γ_s) and the adsorption equilibrium constant (K_{ad}) were calculated to be 0.248 mmol g^{-1} and 1.23 × 10^3 M^{-1}, respectively. The large K_{ad} value indicates that there is strong interaction between the NH_4^+ ion and the FTO surface. Further, the ζ-potential of FTO particles was measured as a function of $[(NH_4)_2SO_4]$ (Fig. 4B). In water (pH 6.1), the FTO particles have a ζ-potential of −10.4 mV, which increases with an increase in $[(NH_4)_2SO_4]$. Also, the

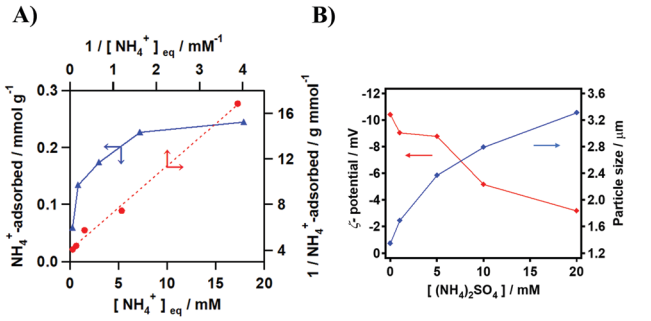

Fig. 4 (A) Adsorption isotherm of NH_4^+ ions on FTO particles at 25 °C. (B) ζ-potential and particle size of ATO particles in aqueous solutions as a function of $[(NH_4)_2SO_4]$ (pH 5.8 ± 0.3).

particle size increases with increasing $[(NH_4)_2SO_4]$ due to the aggregation of the particles. Clearly, NH_4^+ ions are adsorbed on the surface of FTO particles by the Coulomb interaction.

Further, the adsorption state of NH_4^+ ions on FTO from an aqueous solution of $(NH_4)HCO_3$ was studied by diffuse reflectance Fourier-transform infrared (DRIFT) spectroscopy (Fig. S7A, ESI†). After the adsorption, a broad absorption appears around 1440 cm^{-1} due to the deformation of NH_4^+.[20] In addition, two absorptions with the peaks at 1695 cm^{-1} and 1362 cm^{-1} assignable to the anti-symmetric and symmetric stretching vibrations of HCO_3^--ion co-adsorbed with a monodentate structure are observed.[21] Importantly, the absorption peaks for the HCO_3^- ions adsorbed on FTO intensifies in the presence of NH_4^+ ions (Fig. S7B, ESI†). Clearly, the NH_4^+ ions on FTO promote the adsorption of HCO_3^- ions.

On the basis of these results above, a possible action mechanism of the NH_4^+ ion-promoted electrochemical CO_2-RR is proposed (Scheme 1). At the GC cathode, water is oxidized to yield O_2 and H^+ (eqn (5)). On the other hand, the NH_4^+ ions are strongly adsorbed on the FTO surface through Coulomb interaction. At the initial stage of electrolysis, the partial reduction of FTO yields Sn NPs on the surface (eqn (6)). Sn/FTO can act as the active sites for water reduction to generate hydrogen atoms on the surface (eqn (7)) of which coupling produces H_2 (eqn (8)). In parallel with the process,

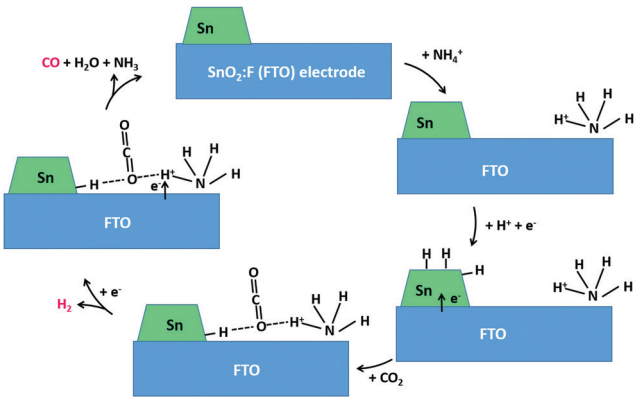

Scheme 1 Action mechanism of the ammonium ion on the electrochemical reduction of CO_2 on the FTO electrode.

HCO_3^- ions or CO_2 (eqn (1) and (2)) can be concentrated near the FTO surface through the hydrogen bonds with NH_4^+ ions. The subsequent electrochemical H^+-coupled electron transfer to CO_2 yields CO and H_2O (eqn (9)).

GC anode:

$$2H_2O \rightarrow O_2 + 4H^+ + 4e^- \quad (5)$$

FTO cathode:

$$SnO_2 + 4H^+ + 4e^- \rightarrow Sn/FTO + 2H_2O \quad (6)$$

$$Sn/FTO + H^+ + e^- \rightarrow Sn\text{-}H/FTO \quad (7)$$

$$2Sn\text{-}H/FTO \rightarrow H_2 + 2Sn/FTO \quad (8)$$

$$CO_2\cdots NH_4^+ + Sn\text{-}H/FTO + e^- \rightarrow CO + H_2O + NH_3 + Sn/FTO \quad (9)$$

The resulting NH_3 extracts H^+ from water to regenerate the NH_4^+ ion. In this case, the pH of the electrolyte solution can be maintained near neutral throughout the electrolysis by the buffering action of HCO_3^- ions in the electrolyte solution (eqn (2)). In this manner, NH_4^+ ions on FTO can promote the adsorption of the HCO_3^- ion or CO_2 (eqn (1) and (2)) on the electrode surface but also work as a proton donor under near-neutral conditions to enhance the CO_2-RR to CO. This scheme may remind one of the catalytic effects of pyridine and derivatives on the photoelectrochemical CO_2-RR to HCOOH at the p-GaP electrode.[22] However, the action mechanism of the present NH_4^+ ion-promoted CO_2-RR seems to be quite different from that in the pyridine-catalyzed CO_2-RR, where the reaction *via* dihydropyridine has recently been proposed.[23] Further experimental and theoretical study is necessary to elucidate the detailed action mechanism.

In summary, this study has shown that a drastic promotion of the electrochemical production of synthetic gas from water and CO_2 on the Sn/FTO cathode is induced by the addition of NH_4^+ ions in the electrolyte solution. In this system, NH_4^+ ions adsorbed on the FTO surface enhance the adsorption of HCO_3^- ions, which can act as a reservoir for CO_2 on Sn/FTO. In addition, the NH_4^+ ions are suggested to be a proton donor in a near-neutral electrolyte solution and a mediator for proton-coupled electron transfer from the cathode to CO_2. We anticipate that this study can be a trigger for the development of the electrochemical production of synthetic gas for CO_2 conversion to value-added chemicals.

The authors acknowledge Prof. M. Fujishima (Kindai University), Dr T. Sento, Mr M. Shima, Mr T. Takahashi, and Mr Y. Sumida (Nippon Shokubai Co.) for helpful discussion. This work was financially supported by the JST Adaptable and Seamless Technology Transfer Program through Target-driven R&D, JSPS KAKENHI Grant-in-Aid for Scientific Research (C) no. and 18K05280 and 20K05674, the Futaba Foundation, and the Nippon Sheet Glass Foundation for Materials Science and Engineering.

Conflicts of interest

There are no conflicts to declare.

Notes and references

1 S. C. Roy, O. K. Varghese, M. Paulose and C. A. Grimes, *ACS Nano*, 2010, **4**, 1259–1278.
2 Y. J. Sa, C. W. Lee, S. Y. Lee, J. Na, U. Lee and Y. J. Hwang, *Chem. Soc. Rev.*, 2020, **49**, 6632–6665.
3 R. E. Blankenship, D. M. Tiede, J. Barber, G. W. Brudvig, G. Fleming, M. Ghirardi, M. R. Gunner, W. Junge, D. M. Kramer, A. Melis, T. A. Moore, C. Moser, D. G. Nocera, A. J. Nozuk, D. R. Ort, W. W. Parson, R. C. Prince and R. T. Sayre, *Science*, 2011, **332**, 805.
4 T. Yamamoto, D. A. Tryk, A. Fujishima and H. Ohata, *Electrochim. Acta*, 2002, **47**, 3327–3334.
5 S. Hernández, M. A. Farkhondehfal, F. Sastre, M. Makkee, G. Saracco and N. Russo, *Green Chem.*, 2017, **19**, 2326–2346.
6 B. M. Tackett, J. H. Lee and J. G. Chen, *Acc. Chem. Res.*, 2020, **53**, 1535–1544.
7 D. L. T. Nguyen, Y. Kim, Y. J. Hwang and D. H Won, *Carbon Energy*, 2020, **2**, 72–98.
8 M. R. Singh, Y. Kwon, Y. Lum, J. W. Ager, III and A. T. Bell, *J. Am. Chem. Soc.*, 2016, **138**, 13006–13012.
9 M. R. Singh, E. L. Clark and A. T. Bell, *Phys. Chem. Chem. Phys.*, 2015, **17**, 18924–18936.
10 R. Shitatsuchi, K. Hongo, G. Nogami and S. Ishimaru, *J. Electrochem. Soc.*, 1992, **139**, 2544–2549.
11 Y. Chen and M. W. Kanan, *J. Am. Chem. Soc.*, 2012, **134**, 1986–1989.
12 Y. Hori, K. Kikuchi and S. Suzuki, *Chem. Lett.*, 1985, 1695–1698.
13 S. Ikeda, T. Takagi and K. Ito, *Bull. Chem. Soc. Jpn.*, 1987, **60**, 2517–2522.
14 M. Azuma, K. Hashimoto, M. Hiramoto, M. Watanabe and T. Sakata, *J. Electroanal. Chem.*, 1989, **260**, 441–445.
15 F. Köleli, T. Atilan, N. Palamut, A. M. Gizir, R. Aydin and C. H. Hamann, *J. Appl. Electrochem.*, 2003, **33**, 447–450.
16 W. J. Dong, J. W. Lim, D. M. Hong, J. Y. Park, W. S. Cho, S. Baek, C. J. Yoo, W. Kim and J.-L. Lee, *Appl. Energy Mater.*, 2020, **3**, 10568–10577.
17 Q. Li, J. Fu, W. Zhu, Z. Chen, B. Shen, L. Wu, Z. Xi, T. Wang, G. Lu, J.-J. Zhu and S. Sun, *J. Am. Chem. Soc.*, 2017, **139**, 4290–4293.
18 S. Anandan and J. J. Wu, *Ultrason. Sonochem.*, 2015, **21**, 1954–1957.
19 M. Tomisaki, S. Kasahara, K. Natsui, N. Ikemiya and Y. Einaga, *J. Am. Chem. Soc.*, 2019, **141**, 7414–7420.
20 V. Busigny, P. Cartigny, P. Philippot and M. Javoy, *Chem. Geol.*, 2003, **198**, 21–31.
21 E.-M. Köck, M. Kogler, T. Bielz, B. Klötzer and S. Penner, *J. Phys. Chem. C*, 2013, **117**, 17666–17673.
22 E. E. Barton, D. M. Rampulla and A. B. Bocarsly, *J. Am. Chem. Soc.*, 2008, **130**, 6342–6344.
23 T. P. Senftle, M. Lessio and E. A. Carter, *ACS Cent. Sci.*, 2017, **3**, 968–974.

